

Wavelet packet transform-based compression for teleoperation

Ahmet Kuzu^{1,2}, Eray A Baran³, Seta Bogosyan^{1,4}, Metin Gokasan¹ and Asif Sabanovic³

Abstract

This paper introduces a codec scheme for compressing the control and feedback signals in networked control and teleoperation systems. The method makes use of Wavelet Packet Transform (WPT) and Inverse Wavelet Packet Transform (IWPT) for coding and decoding operations, respectively. Data compression is carried out in low-pass filter output by reducing the sampling rate, and in high-pass filter output by truncating the wavelet coefficients. The proposed codec works on both directions of signal transmission between a master robot and a slave robot over a networked motion control architecture. Following the formulation of the compression/decompression methodology, experimental validation is conducted on a single-degree-of-freedom motion control system. In the experiments, responses from different Wavelet structures are analyzed and a comparative study is carried out considering the factors of compression rate, reconstruction power error and real-time computational complexity. It is confirmed that the controller using the proposed compression algorithm performs very close to the uncompressed one while enabling transmission of much less data over the network.

Keywords

networked control systems, teleoperation, wavelet packet transform, haptic data compression

Introduction

Recent achievements of robotics technology paved the way through control of multiple robotic systems to accomplish certain tasks together. Teleoperation, referring to the operation from a distant location, is an example of a networking control structure between distant robotic systems. Owing to its potential contribution to applications, such as safety, security, exploration and biomedical sciences, teleoperation systems recently became an active research field. Some examples including the use of robotic systems with networking control include hazardous area explorations, chemical material deposition systems, telesurgery and aerospace applications. The main problem of a teleoperation system is to provide synchronized control of positions and forces between geographically separated motion control systems. In particular, when the Internet medium is used for data exchange, communication delays between the transmitted signals make the motion synchronization problem more difficult.

Signal transmission over the Internet causes problems such as deterioration of stability and controller performance. The problem arises due to the limitations

of network communication and existence of time delay in the Internet medium. Providing robust operation in a networking control system can be feasible only after communication constraints are taken into consideration.¹ In addition to the effect of time delay, the conflicting nature of bandwidth limitations and sampling rate have direct consequences on the performance of the controller and vivid haptic sensation from the remote environment.²

In the literature, several studies have been proven to perform successfully for teleoperation systems. One of the early studies about the time delay problem proposed the use of the Smith Predictor for compensation of the motion in the existence of a constant and known amount of delay.³ A relatively modern approach is

¹Istanbul Technical University, Istanbul, Turkey

²Tubitak, Bilgem, Kocaeli, Turkey

³Sabanci University, Istanbul, Turkey

⁴University of Alaska, Anchorage, AK, USA

Corresponding author:

Ahmet Kuzu, Tubitak, Bilgem, 41470, Kocaeli, Turkey.

Email: ahmet.kuzu@tubitak.gov.tr

adopted by methods utilizing passive signal exchange,^{4,6} and methods based on scattering theory and wave variables.^{7,8} Some recent studies based on impedance adaptation have been shown to perform successfully for better reconstruction of interaction forces of unstructured remote environments on the master side.^{9,10} The stability proofs of these methods have been studied in various settings. However, most of these methods are still lacking in terms of transparency, which is a must in teleoperation systems.¹¹ Besides the solutions using passivity theory and wave variables, methods based on the concept of network disturbance have also been popularized for applications on teleoperation systems.^{12–14} Studies considering the solution of time-delayed motion synchronization problem from a robust acceleration control point of view have been proposed.^{15,16}

In order to quantify the performance of teleoperation systems, some researchers defined certain metrics mostly based on telepresence and transparency.¹⁷ Based on such indices, quantitative and analytical comparisons of some of the methods used for motion control under time delay have been presented in the literature.^{18,19} For further information, the reader is directed to a recent survey.²⁰

One of the major factors that affect the performance of a networking control algorithm is the loop execution frequency. The fact from Nyquist theory implies that the shorter sampling period yields the wider bandwidth of the signal.²¹ The communication infrastructure of a teleoperation system, having consisted of communication lines and router devices, imposes significant limitations on packet transmission rates. Moreover, as a natural drawback of the Internet medium, network congestion risk increases when an interval of packet transmission is shortened. Owing to the network congestion, the amount of communication delay and rate of packet loss increase significantly, which deteriorates the performance of the overall control system. In order to overcome the effects of congestion, some compression-based methods have been proposed that set the frequency of packet transmission lower than that of the control loop.^{2,22,23} Utilization of compression algorithms implies the existence of two Nyquist frequencies for the acquisition of a signal; one that is determined by the sampling period for the control, and the other being determined by the packet transmission rate.

A similar problem can be observed in biomedical sciences when trying to transmit bio-potential signals, such as electrocardiogram (ECG) data, over the network. For those systems, compression schemes are used that implicitly make use of some transformations. Some examples of these compression structures include the discrete cosine transform (DCT), Walsh transform, Karhunen–Loeve transform (KLT), and wavelet transform. The contribution made by using a transformation for compression comes from the ability to concentrate the energy of the original signal in smaller sized data packages. With the particular selection of the transformation scheme, it becomes feasible to represent the

signal by using small number of coefficients in exchange of small losses from the original data.²⁴ In that sense, mappings that would contain more of the energy from the original signal in smaller sized samples would perform better for the compression. The wavelet transform has a good localization property both in time and frequency domains and fits this purpose of the compression idea. Furthermore, by appropriate selection of the wavelet function, representation of the same signal can be obtained with smaller error.

Despite being an important factor influencing performance, the use of compression approaches in the area of teleoperation and networking control are very rare,^{25–27} and are mostly based on DFT and DCT. The novel WPT codec scheme approach proposed by the authors was demonstrated to have a better performance over those approaches in the literature with its capability to track the original signal even at 90% compression rate.²⁸ This is an improved performance over existing compression approaches in the literature. In Kuzu et al.,²⁹ the DFT approach was demonstrated by the authors to have a better performance over DCT, and yet to diverge even at 80% compression rate.²⁸ In addition to its significantly improved performance, another advantage of the proposed WPT approach is its increased flexibility, which allows for a higher number of parameters to be adjusted (i.e. wavelet type, wavelet buffer, vanishing moments, and wavelet level) in comparison to DFT's single adjustment parameter, which is buffer length.

A short packet-sending period and a low communication delay are the main requirements to achieve high synchronization in networking control. However, taking into consideration the bandwidth constraints, there is a tradeoff between the packet-sending period and communication delay. Low-frequency sampling deteriorates the transparency and stability whereas high-frequency excitation of the network increases the possibility of congestion and packet losses.² Making use of compression methods, a flexible design possibility is introduced for adjusting the packet-sending period taking into consideration the bandwidth limitations. Furthermore, since the network jitter is defined as communication delay variation over packet-sending period, use of a compression algorithm in a real-time loop also reduces the jitter disturbing the system from the network.

The main contribution of this study is a detailed performance analysis and experimental verification for the authors' WPT approach²⁸ proposed for teleoperation and networking control applications. To this aim, different wavelet families have been analyzed and experimentally tested at different buffer lengths, wavelet levels, and compression rates, also considering computational cost. The analysis is based on the teleoperation system which was also used in the evaluation of the DFT and DCT approaches in the previous studies.²⁹

The organization of the paper is as follows. Section 2 describes the general scope of networking control

system and bandwidth problem along with an exiting method used for compensation of time delay. Section 3 introduces the WPT while in Section 4, most commonly used basis functions of Discrete Wavelet Transform (DWT) are summarized. Section 5 discusses the WPT-based compression/decompression idea utilized for networking control. Finally, in Sections 6, 7 and 8, results acquired from the experimental case studies, analytical discussion over experiment results and concluding remarks are presented, respectively.

Networking control and bandwidth problem

Networking control refers to the control of a master–slave structure-based robotic system in order to synchronize the position and/or force responses of the robots used within. Teleoperation, in that context, refers to the process of operation in a distant location. Having mentioned a remote environment, one major problem in networking control is the difficulty of satisfying motion synchronization requirement via data transmission over the Internet. The conventional structures of data transmission contain the use of protocols such as UDP/IP and TCP/IP which are subject to transmission delays of unpredictable magnitude. Under these conditions, the control problem takes the form of a variable time delay impedance control problem, which is even a more challenging one than the static time delay control problem.

When network within the control loop is taken into consideration, the trade-off between bandwidth and sampling starts to play a more important role in the system. The uncertain and unstructured form of network medium can yield problems related to variable magnitude transmission delays, or in certain settings of the network (such as UDP/IP), problems due to package losses. For such circumstances, reducing the sampling rate of data sent through the network can improve the performance by reducing the delays and package losses in the loop. However, in order to maintain stable operation, high-frequency sampling is inevitable for the overall control system. In particular, rapidly changing signals such as the input current or reaction force measurement is affected negatively from lowered sampling frequency, which results in degradation of performance for the entire control loop. One good example of performance loss can be seen while having force measurements for hard-contact (i.e. interaction between environments with high stiffness) force control operation.

In order to solve the conflicting behavior of sampling ratios within the system, researchers proposed to use compression/decompression (codec) algorithms for data transmission over the network.^{21,26} Benefiting from codec structure, one can increase the loop frequency of the control system while preserving the data transmission frequency at respectively low values. The

new scheme presented in the context of this paper is based on this down-sampling idea and uses a WPT-based compression scheme. Below, a brief overview of the controller used for the verification of the proposed algorithm is presented.

The time-delayed motion control algorithm utilized for this study makes use of the concept of network disturbance and is based on the controller structure presented in Natori et al.,¹⁴ namely the Communication Disturbance Observer (CDOB). In CDOB structure, the effect of delay in the measurement channel is lumped under the term network disturbance which acts in the acceleration dimension. Hence, in the background, the master and slave plants implicitly makes use of acceleration control framework. Below a brief overview of the system and controller used in this study is presented.

System definition

In the following analysis, the demonstration of the controller will be made on a single-degree-of-freedom (DOF) system. Without loss of generality, one can represent the dynamics of a single-DOF system as

$$a_n \ddot{q}(t) = \tau(t) - \tau_{dis}(t) \quad (1)$$

where a_n and $\tau_{dis}(t)$, respectively, denote the nominal plant inertia and disturbance torque acting on the plant for which generalized coordinate of motion is represented by $q(t)$. Assuming small variations around the linear region, one can write down the input torque as a scalar multiple of the input current and nominal torque constant (i.e. $\tau(t) = K_n i_c(t)$). Substituting this back to equation (1) gives the following

$$a_n \ddot{q}(t) = K_n i_c(t) - \tau_{dis}(t) \quad (2)$$

In equation (2), the term τ_{dis} combines all undesired effects, namely the viscous friction ($b(q, \dot{q})$), deviations from the nominal values for torque constant (ΔK_n) and inertia (Δa_n), effect of gravity ($g(q)$) and all other external torques (τ_{ext}) acting on the system. Hence, the content of $\tau_{dis}(t)$ can be given as

$$\tau_{dis} = \Delta a_n \ddot{q} + \Delta K_n i_c + b(q, \dot{q}) \dot{q} + g(q) + \tau_{ext} \quad (3)$$

In order to use the plant in acceleration control framework, one has to estimate and compensate the disturbance term given in (3). This ideal behavior can be realized via the integration of a Disturbance Observer (DOB) with the remote plant³⁰ either alone, or with additional compensation if further precision is required.³¹

Motion compensation with time delay

When there is delay in either control or measurement channels, real-time signal transmission is hindered. In particular, due to the delays in measurement channel, the controller cannot acquire the information of the

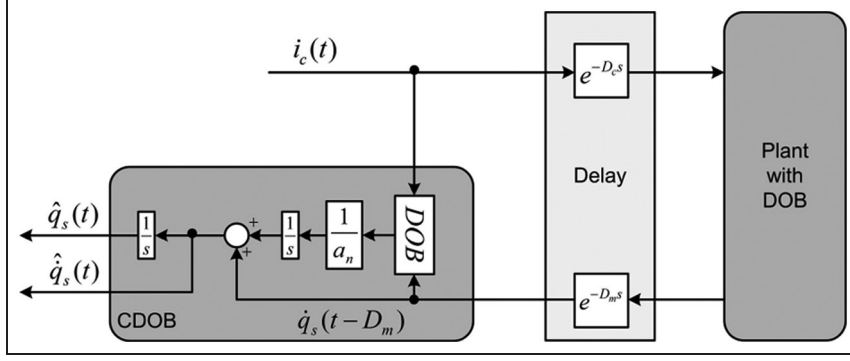


Figure 1. Structure of a network controller.

remote system states and hence cannot generate necessary and correct control input on time which leads an unstable behavior. Further, additional delay in the control channel also contributes negatively on the synchronized motion of master and slave systems.³² The stable operation of the controller can only be ensured if correct estimates of the remote system states can be done. The estimation structure used in the context of this study is the CDOB.¹⁴ In the CDOB structure, the effect created by the measurement delay is considered as a disturbance in acceleration dimension which can be modeled as

$$\tau_{dis}^{mw}(t) = K_n i_c(t) - a_n \ddot{q}_s(t - D_m) \quad (4)$$

where $\tau_{dis}^{mw}(t)$ represents the network disturbance, D_m stands for the delay in the measurement channel, $q_s(t)$ represents the remote system (i.e. slave system) position and $i_c(t)$ represents the control current sent from the master side over the network. The observer implicitly assumes that the slave plant is enforced to behave ideally with nominal torque constant, K_n , and nominal inertia, a_n , due to a disturbance observer as explained in the previous section. Having assumed the nominal behavior of the remote system, the network disturbance can be estimated with another DOB which is termed as the CDOB due to obvious reasons.

The estimated network disturbance stands for the torque that is supposed to act on the slave plant during measurement delay. Since the remote plant is enforced to behave nominally with DOB, the estimated network disturbance can be divided by the corresponding nominal inertia and be integrated to give the velocity difference that is supposed to exist during the measurement delay time. Mathematically, we have

$$\Delta \dot{q}_s(t) = \frac{1}{a_n} \int_0^t \tau_{dis}^{mw}(\varphi) d\varphi \quad (5)$$

The addition of this velocity difference to the delayed slave velocity gives the estimated velocity of the slave plant as shown below

$$\hat{\dot{q}}_s(t) = \dot{q}_s(t - D_m) + \Delta \dot{q}_s(t) \quad (6)$$

The depiction of CDOB structure is given in Figure 1. Further information about CDOB can be found in Natori et al.,^{12,13} whereas a convergence and stability analysis is given in Šabanovic et al.¹⁵

The system compensated with the CDOB structure exhibits a stable behavior with the estimation of the real-time slave motion measurement. In other words, CDOB converts the overall system to one without the measurement delay. Using the estimation from CDOB, the master side controller can generate the necessary input reference that is supposed to act on the slave system after the input channel delay.

Wavelet packet transform

In time-series, analysis can be handled by either in time domain perspective such as moments and correlations or can be handled in the frequency domain perspective such as energy spectra of signals. Wavelets yield a way to analyze these signals both in time and frequency domains by producing local spectral information about them.³³ Unlike the Fourier-based waves, which covers the whole time axis, wavelets are localized in a bounded interval of time which satisfies a few requirements. This flexibility enables construction of new wavelets for new applications. The information from which the signal can be analyzed and reconstructed in the selected time and frequency span can be contained in the wavelet coefficients. Due to their advantages in providing local information, wavelets have been adopted to perform efficiently in many applications like identification and estimation.³⁴

Wavelets are defined by the wavelet function, $\psi(t)$ also called the mother wavelet and scaling function, $\phi(t)$, also called the father wavelet in the time domain. From a practical point of view, wavelet function acts like a band-pass filter with scaling. Hence, in order to cover the entire signal spectrum, one has to use an infinite number of wavelets. Mathematically speaking, the fundamental form of wavelets can be given as follows

$$\psi(t) = \sqrt{2} \sum_{n \in \mathbb{Z}} g(n) \phi(2t - n) \quad (7)$$

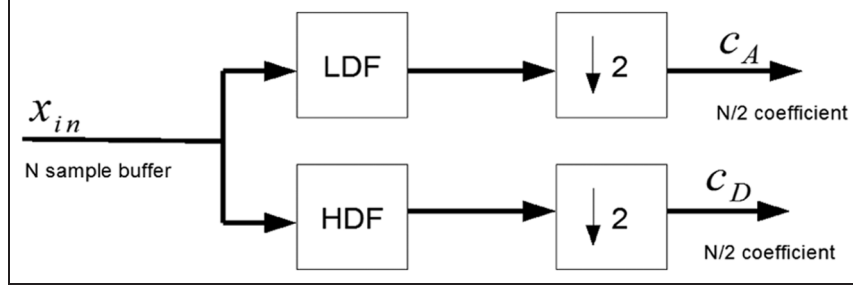


Figure 2. Wavelet decomposition algorithm. Here, LDF denotes low-pass decomposition filter and HDF denotes high-pass decomposition filter which are orthogonal to each other, “↓” operator denotes the down-sampling process, c_A denotes approximate wavelet coefficients and c_D denotes detailed wavelet coefficients. We will call this one-level DWT in the rest of the paper as DWT I.

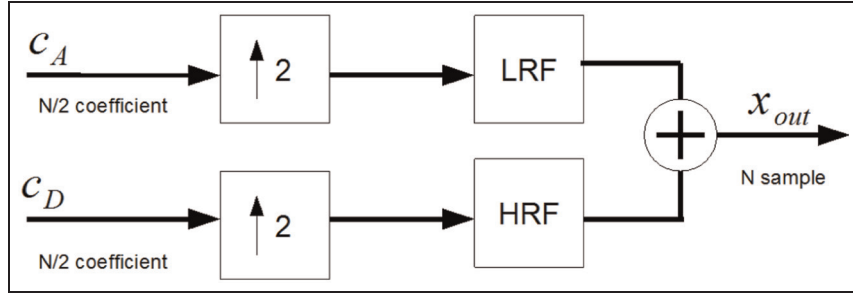


Figure 3. Wavelet reconstruction algorithm. Here, LRF and HRF represent the low-pass reconstruction filter and high-pass reconstruction filter, respectively, which are again orthogonal to each other, and likewise “↑” operator denotes the up-sampling process. Similar to the forward case, this one-level inverse DWT will be abbreviated as IDWT I in the context of this paper.

$$\phi(t) = \sqrt{2} \sum_{n \in \mathbb{Z}} h(n) \phi(2t - n) \quad (8)$$

where $g(n)$ and $h(n)$ stand for the high-pass and low-pass filters, respectively, which together constitute a pair of conjugate quadrature filters (CQFs).³⁵

Application of wavelets on practical systems is very similar to the realization of sub-band coders. In this approach, the signal is separated into low- and high-frequency parts that are called approximation and detail, respectively. In 1988, Mallat produced a fast wavelet decomposition and reconstruction algorithm.³⁶ The Mallat algorithm for DWT is a two-channel sub-band coder which uses CQFs or quadrature mirror filters (QMFs). The one-level DWT algorithm, which is usually denoted as the decomposition algorithm, is shown in Figure 2.

The inversion of the process is similar to the forward case and can be done by just exchanging down-sampling to up-sampling and quadrature filters to QMFs as shown in Figure 3.

DWT basis functions

In wavelet transform, the acquisition of information localized within the signal is dependent on the selection of the basis functions (i.e. wavelets). Based on the structure hidden in the basis function, the information is retrieved via dilations and shifting operations. For convenience of the reader, we provide below a brief

summary of the most commonly used DWT basis functions. The derivations and construction procedures of these wavelets require a much deeper discussion, which is beyond the scope of the work presented here.

Haar

Haar wavelet family is combination of a sequence of square-shaped functions scaled to construct a basis for transformation.³⁷ The mother function $\psi(t)$ and the corresponding scaling function $\phi(t)$ for the Haar wavelet family can be given as follows

$$\psi(t) = \begin{cases} 1 & 0 \leq t < 1/2 \\ -1 & 1/2 \leq t < 1 \\ 0 & \text{otherwise} \end{cases} \quad (9)$$

$$\phi(t) = \begin{cases} 1 & 0 \leq t < 1 \\ 0 & \text{otherwise} \end{cases} \quad (10)$$

Coiflets

Coiflets constitute another set of discrete wavelet basis functions which have scaling functions with vanishing moments.³⁸ Mathematically, the mother and scaling functions of generalized Coiflet of order l (denoted as $\psi_{l,\mu}$ and $\phi_{l,\mu}$) for some $\mu \in \mathbb{R}$, is supposed to satisfy

$$\int_{\mathbb{R}} t^p \psi_{l,\mu}(t) dt = 0 \quad (11)$$

$$\int_{\mathbb{R}} (t - \mu)^p \phi_{l,\mu}(t) dt = \delta_p \quad (12)$$

where $p = 0, 1, \dots, l-1$ and μ is the center of mass of scaling function $\phi_{l,\mu}(t)$.³⁵

Daubechies

Daubechies family constitute an orthogonal wavelet basis which is characterized by a maximum amount of vanishing moments for some given support N . Unlike other wavelets, in Daubechies wavelets the mother function is dependent on the scaling function and the scaling function can be obtained from a recursion equation.³⁹ Mathematically, for $N \in \mathbb{N}$, Daubechies wavelet of class D- $2N$ can be obtained from the following mother and scaling functions

$$\psi(x) = \sqrt{2} \sum_{k=0}^{2N-1} (-1)^k h_{2N-1-k} \phi(2x - k) \quad (13)$$

$$\phi(x) = \sqrt{2} \sum_{k=0}^{2N-1} h_k \phi(2x - k) \quad (14)$$

where $h_0, h_1, \dots, h_{2N-1}$ are the constant coefficients of filter satisfying the following conditions

$$\sum_{k=0}^{N-1} h_{2k} = \sum_{k=0}^{N-1} h_{2k+1} = \frac{1}{\sqrt{2}} \quad (15)$$

$$\sum_{k=2l}^{2N-1+2l} h_k h_{k-2l} = \begin{cases} 1 & \text{if } l = 0 \\ 0 & \text{if } l \neq 0 \end{cases} \quad (16)$$

with $l = 0, 1, \dots, N-1$. As obvious from equation (13), in order to obtain the wavelet, first the recursion given in equation (14) has to be solved for $x \in \mathbb{R} \setminus [0, 2N-1]$.

Bior

The biorthogonal wavelet family differs from the function side since they are not based on vanishing moments.⁴⁰ Mathematically, the form of the corresponding mother and scaling functions⁴¹ for Bior wavelet family can be given as

$$\psi(t) = \sum_{k=0}^N 2g^r(k) \phi(2t - k) \quad (17)$$

$$\phi(t) = \sum_{k=0}^N h^r \phi(2t - k) \quad (18)$$

where $g^r(k)$ and $h^r(k)$ stand for the reverse of the original filters $g(k)$ and $h(k)$, respectively.

Rbior

Reverse biorthogonal wavelet functions are generated by interchanging decomposition and reconstruction filters of the original biorthogonal wavelet functions. The mother and scaling functions of these wavelets share the same mathematical representation with the original biorthogonal wavelets as given in equations (17) and (18), respectively.

The variations between the wavelet functions result in differences in terms of compression rates and computational complexities introducing a pay-off to select the best wavelet function for the particular application in hand. The dependency of compression rate is more closely related to the shape of the signal being compressed and the shape of the wavelet used for the transformation. In order to provide a consistent analysis of the selected wavelets, the general shapes of these wavelets and the information related to their buffer sizes are provided in Figures 4 and 5, respectively.

WPT-based compression system for networking control

The wavelet packet method involves decomposing the signal using wavelets in binary tree form. For the selected orthogonal wavelet function (LDF and HDF), we generate a set of bases called wavelet packet bases. Every set has particular features of the original signal. The wavelet packets can be used for lots of expansions of a given signal.

In the orthogonal wavelet decomposition procedure, the approximation coefficients are always separated into two parts, resulting in a vector of approximation coefficients and a vector of detail coefficients, both of which work at a coarser scale. Then, the approximation coefficient vector is separated again, but details are not reanalyzed anymore. Hence, the information loss is in the detailed side. In the case of wavelet packet transmission, both detail and approximation coefficient vectors are separated, hence offering the richest analysis

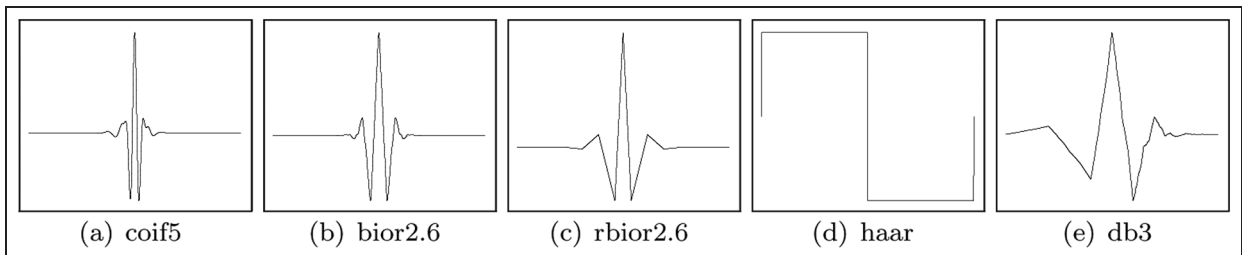


Figure 4. General shapes of wavelet basis functions.

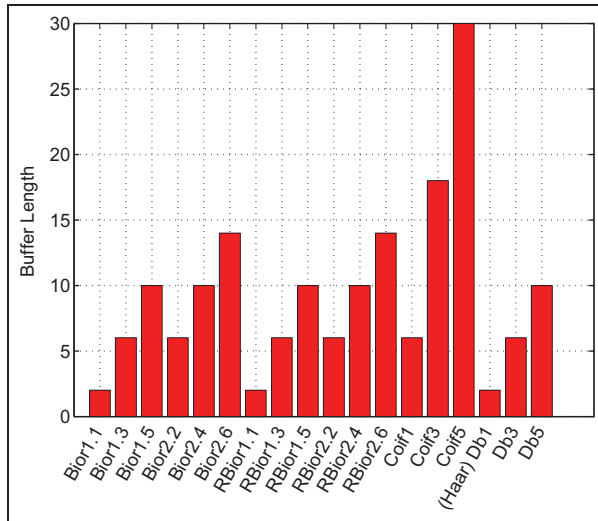


Figure 5. Buffer length of wavelets.

capability. The complete binary tree is produced in this way as given in the Figure 5(A) and (B).

In the WPT-based compression architecture, wavelet packet tree system is used to decompose and reconstruct the signal. Once again, the signal is separated into its low- and high-frequency parts. Following this separation, the low-frequency component of the signal is down-sampled and the high-frequency component of the signal is compressed according to algorithm which saves the predefined amount of maximum wavelet component and cancels others.

For the decompression process, the low-frequency part and high-frequency components are decompressed separately and then combined together. It is adequate to hold each sample of low-frequency signal for N times. For decompression of the high-frequency side, the inverse wavelet packet transform is applied to the wavelet packet tree. The selection process means saving maximum predefined amount of components. Having acquired the two components constituting the original signal, low-frequency components are summed with decompressed high-frequency signals and the recovery of the original data is completed. The whole process is shown in Figure 7.

Experimental results

The experimental validation for the proposed compression scheme is performed on an experimental setup including linear direct drive motors used for the realization of networking control. The experimental platform consisted of two Hitachi-ADA series linear AC motors and drivers equipped with Renishaw RGH41 type incremental encoders that has $1 \mu\text{m}$ resolution. The algorithm is compiled from a C code and real-time processing is executed by a D-Space DS1103 card.

In the experiments, artificially generated time delays that have constant and varying components in both

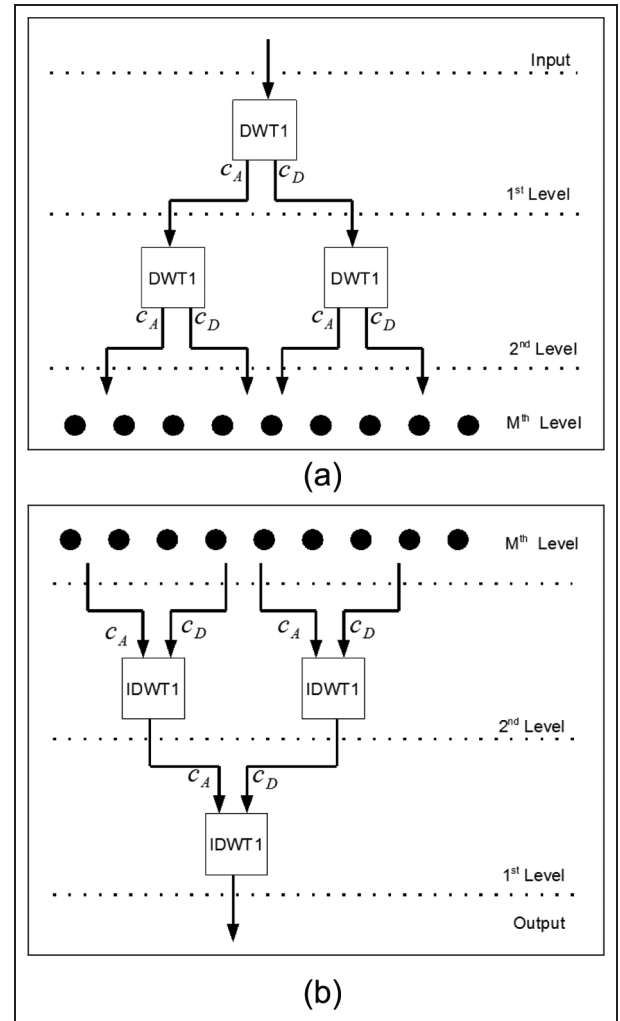


Figure 6. Wavelet packet transform tree: (A) decomposition; (B) reconstruction.

measurement and control channels are employed between master and slave operators. During experiments, the compression and decompression is made using the WPT-based compression algorithm running in various parameter sweep conditions to test their effects on the overall performance. These conditions include wavelet family, compression level (i.e. depth), buffer size and compression ratio. A picture of the experimental setup is given below in Figure 8.

In the experiments, the master operator is computer controlled with sinusoidal position reference and the corresponding control current $i_c(t)$ from the same sine position tracking command is used in the compression algorithm since in networking control, the control current of the master system is the primary data that is sent to the remote system. Selection of the input current has one more important aspect. Since current input is the fastest varying signal within the control loop (i.e. the signal for which high-frequency components carry the most important information) the performance of the compression algorithm can best be seen on this data. Figure 9 shows one segment of the compressed control

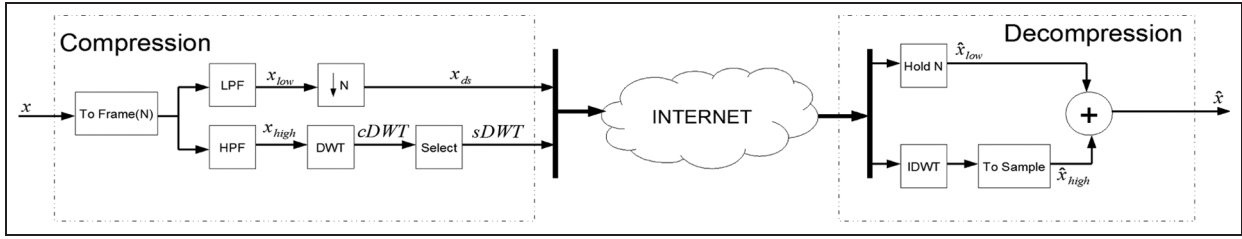


Figure 7. Proposed DWT-based compression–decompression scheme.

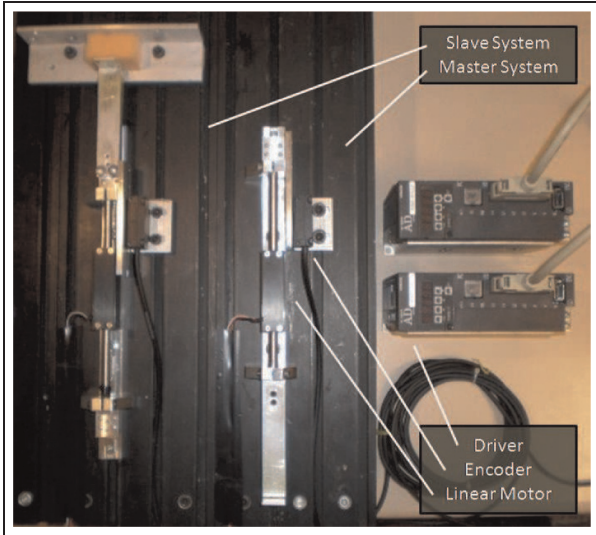


Figure 8. Experimental setup.

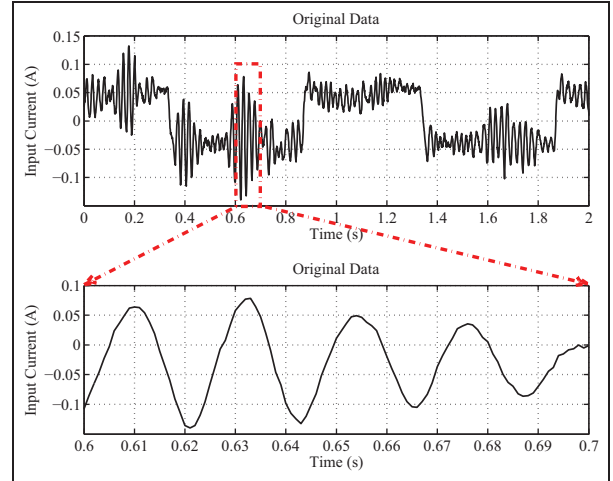


Figure 9. Original signal used for compression–decompression.

current while the detailed plots obtained by zooming on the marked region is provided over the same figure.

In order to have better evaluation of performance, power error comparisons are made using the same signals for every different scenario. For each case, the compression ratio is changed from 0% to 100% and the results are plotted with respect to the following power error E_P :

$$E_P = \frac{P_{Original} - P_{Decomposed}}{P_{Original}} \times 100 \quad (19)$$

where $P_{Original}$ and $P_{Decomposed}$ respectively stand for the power of original and decomposed signals.

Since the number of parameters that affect the overall algorithmic performance are relatively high, here we adopt a methodological way to observe the effects of these parameters by carrying out separate analysis for each different factor. For that purpose, three different experiment sets are carried out and explained below.

Experiment set I

The first experiment set covers analysis with respect to the wavelet family and compression depth for which the results are given in Figure 10. In these figures, the main objective is to see the change in responses via changing the vanishing moments of the corresponding

family and changing the compression depth (i.e. level) under constant vanishing moment of the corresponding family. The families used in the experiment content include Biorthogonal 1.x, Biorthogonal 2.x, Reverse Biorthogonal 1.x, Reverse Biorthogonal 2.x, Coiflets and Daubechies, given in Figure 10(a)–(f), respectively. In these figures, for each family, the upper subfigure shows the effect of the family parameter on the power error with respect to the comparison ratio and the lower subfigure shows the effect of wavelet depth on the power error with respect to the comparison ratio.

Referring to the upper subfigures, one can conclude that the compression error decreases slightly with increasing vanishing moments for every wavelet family. On the other hand, the computational complexity comes into picture when talking about increasing vanishing moments since that means increasing the length of reconstruction and decomposition filters as seen in Figure 5. Hence, one has to take into consideration the relative change in the required computational power for a small enhancement in the compression performance.

On the other hand, having observed the lower subfigures, one can deduce that increasing the wavelet depth results in better performance regardless of the wavelet structure. This result is consistent with the intuitional expectation, since at every additional level more coefficients are generated to represent the same signal. However, here again one has to consider the increasing computational complexity with the increasing depth.

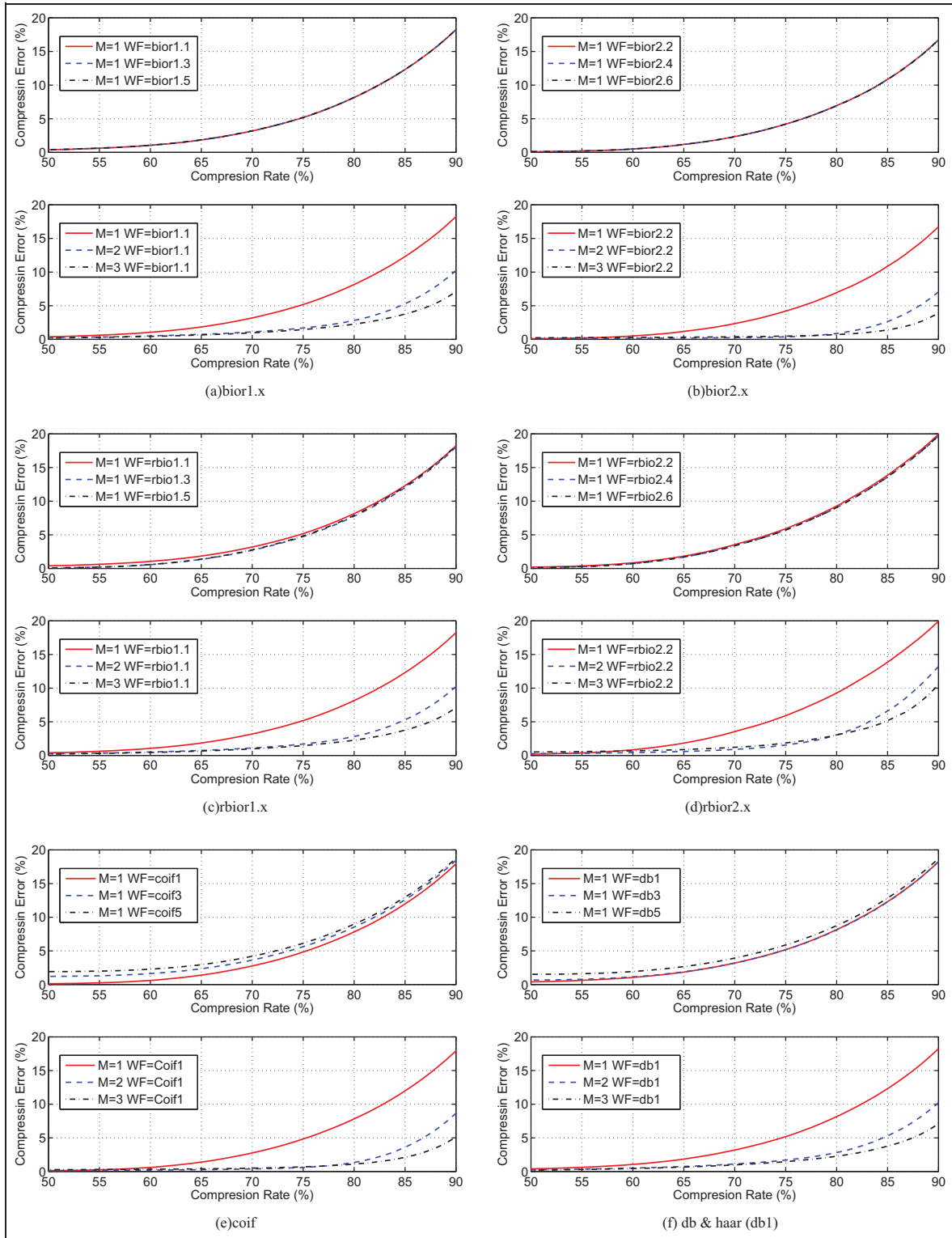


Figure 10. Comparison of wavelet families with respect to vanishing moments and compression levels.

Theoretically the computational requirements double as the compression depth is increased one step forth. Hence, selection of compression depth is a matter of decision based on the available computational power that can be permitted by the real-time processing unit under certain sampling time constraint.

Experiment set 2

Another set of experiments is made to observe the relationship between compression ratio and the size (i.e. length) of buffer used for storing and reconstructing the data under constant compression depth for wavelet families Biorthogonal 2.6, Reverse Biorthogonal 2.6,

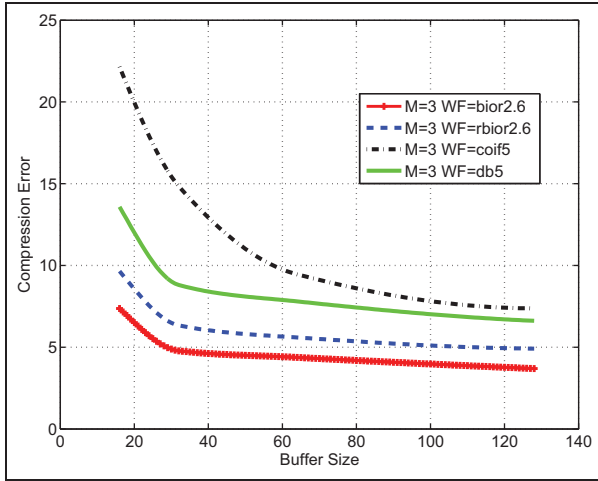


Figure 11. Comparison of wavelet families with respect to buffer size.

Coiflets 5 and Daubechies 5. Once again reconstruction power error is taken as the major metric to analyze the results which are shown in Figure 11. In this experiment set, the buffer length used in the algorithm is swept from 16 to 128 and the compression rate is kept at 90% for all wavelet families.

The results obtained from this experiment set show that the reconstruction error decays exponentially as the buffer size is increased. In other words, increasing buffer length after a certain point has almost negligible effect on the overall reconstruction performance of the signal. On the other hand, just like the compression depth, having larger buffer means increased computational cost.

Another important result obtained from Figure 11 is the considerable change of reconstruction error between wavelet families. For the entire sweep range of buffer size, Bior family outperforms the other wavelet bases while the worst results are obtained from Coiflet family. Having considered the simpler structure of Bior with respect to other families, one can conclude that it comes out as the best selection for the entire range of buffer length.

Experiment set 3

The final set of experiments includes a comparison between the wavelet families with respect to power error under constant buffer size and constant level of compression. For that purpose, results obtained from families Biorthogonal 2.6, Reverse Biorthogonal 2.6, Coiflets 5, and Daubechies 5 are compared and shown in Figure 12 all of which having buffer size equal to 128 and compression depth being equal to 3.

Based on the results shown in the figure, one can conclude that in terms of error performance, Bior family once again give the best response while Coiflet family performs worst. Families Rbior and Daubechies show intermediate responses. However, here one can

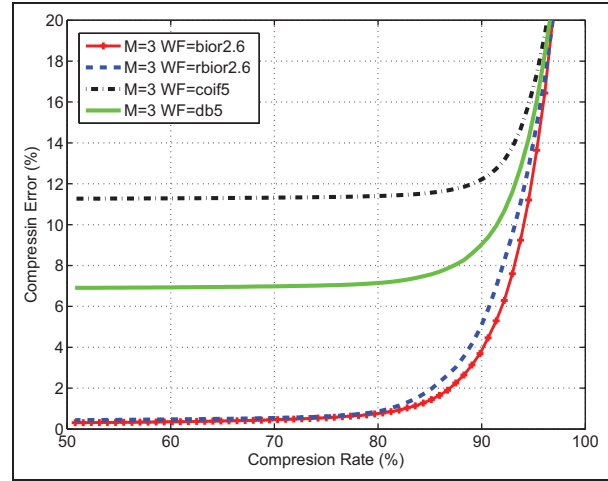


Figure 12. Comparison of wavelet families with respect to compression ratio.

also observe that for low ranges of compression, Rbior family gives almost the same response with Bior bases.

Discussion

Having evaluated the results shown in these experiments, few important conclusions can be summarized. The first result is the negligible effect of vanishing moments on the performance of the system. Since vanishing moments add up with further computational complexity, for realization of the given framework, it is recommended to take the vanishing moments with the least complexity. The second remarkable conclusion that can be observed from the system is improvement of performance with increasing compression depth. Based on the results, selection of compression depth at the level $M = 3$ seems to be a good solution as compression rates of 85% can be achieved within the error bounds of 5% with relatively low computational requirement. Another result obtained from the experiments indicate that increasing buffer size contributes on the reconstruction performance in an exponentially decaying manner. On the other hand, like the vanishing moments and compression depth, buffer size also negatively affects the computational requirements of the system. As the computational requirements increase linearly with increasing buffer size, one can make a relatively easier selection. From the given results, a buffer size of 64 seems to be a good selection for networking control application. The final result that can be acquired from the last experiment set indicates that the reconstruction error remains same for most of the range of compression ratios. However, increasing the compression ratio beyond values of 80%, the power error starts to rise up exponentially with compression rate for all families. Having summarized all of these results, a meaningful selection of the system configuration for the proposed WPT-based compression scheme will be using the basis family Bior2 with the first

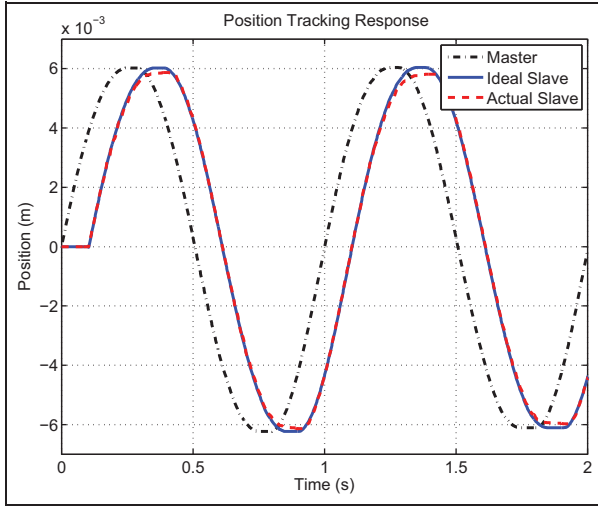


Figure 13. Position tracking responses of the master and slave systems.

vanishing moment (i.e. Bior2.2) and with compression depth of $M = 3$ and buffer size of 64.

In order to better illustrate the performance of the compression algorithm, the position responses of the master and slave manipulators are recorded and shown in this section. For that purpose, the master system is operated under a computer-controlled sinusoidal position reference and the compressed control current is sent to the slave system over an artificially generated network delay of varying magnitude between 95 and 105 ms. Following the discussion on the results obtained from experiments, the WPT-based compression algorithm is tuned to have the configuration described at the end of the previous paragraph. The decompressed control signal is then used to drive the slave system based on the time-delayed motion control algorithm described in Section 2. In order to observe the performance of the proposed codec scheme in real-time control, the original master position signal is also transferred through the same amount of delay and plotted together with the actual slave position response under the label “Ideal Slave” as shown in Figure 13.

As obvious from the given plots, the proposed WPT-based algorithm performs efficiently in compressing and decompressing the high-frequency signals being used in network delayed teleoperation systems. For the sake of completeness, the actual slave motion data is analyzed in terms of power error with respect to the ideal slave motion data using the power error defined in equation (19). It turns out that the power error between ideal and actual slave motion is 4.81% meaning that the recovery of original data is made with an accuracy level above 95%. It should also be pointed out here that this error contains both the error due to the imperfections of estimation in network delayed control algorithm (Section 2) and the error due to compression and decompression in WPT-based algorithm. Hence, the proposed algorithm alone is supposed to perform even better if all imperfections in the system are cleared out.

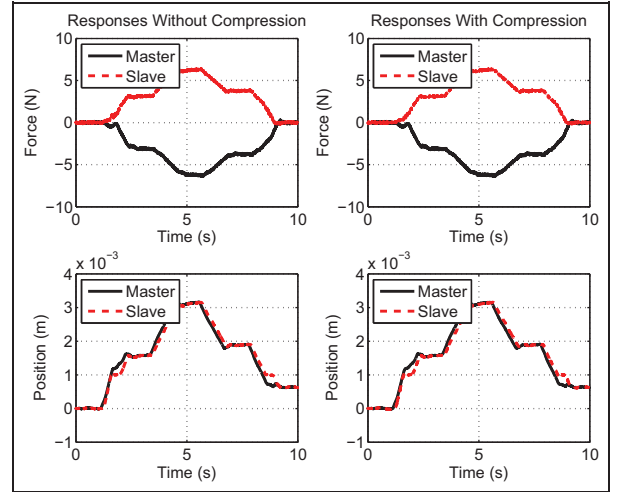


Figure 14. Wavelet position and force tracking results under soft contact.

In order to show the effect of compression on transparency, the position and force responses of the master and slave manipulators are recorded making use of the proposed codec scheme and above-mentioned network controller. For that purpose, the master system is first moved by a human operator and the corresponding motion is recorded. Then, this recorded motion is given as reference to master system under a computer-controlled loop and the slave system is home positioned to have contact with remote environment. While, in the first scenario neither position nor force signal is compressed, in the second scenario both position and force signals are compressed and decompressed. The results are shown in Figure 14. From the given figure, it is obvious that the effect of the proposed compression algorithm is negligible on the overall response of the system. However, in the experiment contact to soft material is tested, because in the hard contact without compression case, the performance is still low, oscillation occurs. So that it does not seem meaningful to compare that case with its compressed version.

Conclusion

In this study, a compression–decompression algorithm using wavelet packet transform is proposed as a novel approach for networked control and teleoperation systems. The derivation of the proposed codec scheme is followed by a detailed analysis of the factors and parameters affecting the performance of the system. For the convenience of the reader, brief summaries are provided for the controller structure and the wavelet families that are used in the context of this study. Detailed experimental results are evaluated in a comparative manner and several conclusions are drawn to utilize the algorithm in teleoperation with the best possible performance. Network control systems can benefit from compression approaches due to the fact that compression allows for sampling rates that are higher than the

network throughput by a multiple of the compression ratio. Moreover, this is achieved with very little loss in the control input power. The authors have already emphasized the benefits of this proposed novel compression approach comparatively with respect the DCT- and DFT-based compression approaches in the literature.^{25–27} Different from previous studies, this paper performs a comprehensive analysis of the novel compression approach in terms of its parameters and how they affect the system. Our analysis verified that increasing the buffer length affects the compression performance positively, while also increasing the network delay, as expected from compression approaches in general. The analysis performed among different wavelet families in terms of different parameters demonstrated the biorthogonal wavelets to have the best performance. An interesting conclusion was reached with another wavelet parameter known as vanishing moment, which, while increasing computational complexity, was observed to have little or no effect on the system performance. The compression depth, on the other hand, was noted to improve performance. Consideration of the above outcomes favors the selection of wavelets with optimum buffer size, maximum compression depth, and a vanishing moment with minimum complexity.

Funding

This work was supported by TUBITAK (projects 111M359 and 110M425) and TUBITAK-Bideb.

References

- 1 Heemels WH, Teel AR, van de Wouw N, et al. Networked control systems with communication constraints: Tradeoffs between transmission intervals, delays and performance. *IEEE Trans Automatic Control* 2010; 55(8): 1781–1796.
- 2 Yashiro D and Ohnishi K. Performance analysis of bilateral control system with communication bandwidth constraint. *IEEE Trans Indust Electron* 2011; 58(2): 436–443.
- 3 Smith OJ. A controller to overcome dead time. *ISA Journal* 1959; 6(2): 28–33.
- 4 Anderson R and Spong MW. Bilateral control of teleoperators with time delay. *IEEE Trans Automatic Control* 1989; 34(5): 494–501.
- 5 Ryu JH, Kwon DS and Hannaford B. Stable teleoperation with time-domain passivity control. *IEEE Trans Robotics Automation* 2004; 20(2): 365–373.
- 6 Ryu JH and Preusche C. Stable bilateral control of teleoperators under time-varying communication delay: time domain passivity approach. In *2007 IEEE international conference on robotics and automation*. IEEE, pp. 3508–3513.
- 7 Niemeyer G and Slotine JJ. Stable adaptive teleoperation. *IEEE J Oceanic Eng* 1991; 16(1): 152–162.
- 8 Niemeyer G and Slotine JJE. Telemanipulation with time delays. *Int J Robotics Res* 2004; 23(9): 873–890.
- 9 Daly JM and Wang DW. Time-delayed bilateral teleoperation with force estimation for n -dof nonlinear robot manipulators. In *2010 IEEE/RSJ international conference on intelligent robots and systems (IROS)*. IEEE, pp. 3911–3918.
- 10 Love LJ and Book WJ. Force reflecting teleoperation with adaptive impedance control. *IEEE Trans Syst Man Cybernet B* 2004; 34(1): 159–165.
- 11 Lawrence DA. Stability and transparency in bilateral teleoperation. *IEEE Trans Robotics Automation* 1993; 9(5): 624–637.
- 12 Natori K and Ohnishi K. A design method of communication disturbance observer for time-delay compensation, taking the dynamic property of network disturbance into account. *IEEE Trans Indust Electron* 2008; 55(5): 2152–2168.
- 13 Natori K, Oboe R and Ohnishi K. Analysis and design of time delayed control systems with communication disturbance observer. In *IEEE international symposium on industrial electronics, 2007 (ISIE 2007)*. IEEE, pp. 3132–3137.
- 14 Natori K, Tsuji T and Ohnishi K. Time delay compensation by communication disturbance observer in bilateral teleoperation systems. In *9th IEEE international workshop on advanced motion control (2006)*. IEEE, pp. 218–223.
- 15 Šabanovic A, Ohnishi K, Yashiro D, et al. Motion control systems with network delay. *AUTOMATIKA* 2010; 51(2): 119–126.
- 16 Sabanovic A, Ohnishi K, Yashiro D, et al. Motion control systems with network delay. In *35th annual conference of IEEE industrial electronics, 2009 (IECON'09)*. IEEE, pp. 2277–2282.
- 17 Willaert B, Reynaerts D, Van Brussel H, et al. Bilateral teleoperation: Quantifying the requirements for and restrictions of ideal transparency. *IEEE Trans Control Syst Technol* 2014; 22(1): 387–395. DOI:10.1109/TCST.2013.2251345.
- 18 Rodriguez-Seda EJ, Lee D and Spong MW. An experimental comparison study for bilateral Internet-based teleoperation. In *Computer Aided Control System Design, 2006 IEEE International Conference on Control Applications, 2006 IEEE International Symposium on Intelligent Control*. IEEE, pp. 1701–1706.
- 19 Sankaranarayanan G and Hannaford B. Experimental comparison of internet haptic collaboration with time-delay compensation techniques. In *IEEE international conference on robotics and automation, 2008 (ICRA 2008)*. IEEE, pp. 206–211.
- 20 Hokayem PF and Spong MW. Bilateral teleoperation: An historical survey. *Automatica* 2006; 42(12): 2035–2057.
- 21 Mizuochi M and Ohnishi K. Coding and decoding scheme for wide-band bilateral teleoperation. In *Advanced Motion Control (AMC), 2012 12th IEEE International Workshop on*. IEEE, pp. 1–6.
- 22 Kuschel M, Kremer P and Buss M. Passive haptic data-compression methods with perceptual coding for bilateral presence systems. *IEEE Trans Syst Man Cybernet A* 2009; 39(6): 1142–1151.
- 23 Lee Jy and Payandeh S. Performance evaluation of haptic data compression methods in teleoperation systems. In *2011 IEEE World Haptics Conference (WHC)*. IEEE, pp. 137–142.
- 24 Yokokura Y, Katsura S and Ohishi K. Bilateral control using compressor/decompressor under the low-rate communication network. In *IEEE international conference on Mechatronics, 2009 (ICM 2009)*. IEEE, pp. 1–6.

- 25 Tanaka H and Ohnishi K. Haptic data compression/decompression using DCT for motion copy system. In *IEEE international conference on Mechatronics, 2009 (ICM 2009)*. IEEE, pp. 1–6.
- 26 Tanaka H, Ohnishi K and Nishi H. Implementation of lossy haptic data compression using integer DCT to FPGA. In *IECON 2010 - 36th annual conference of the IEEE Industrial Electronics Society*. IEEE, pp. 1726–1731.
- 27 Yokokura Y, Katsura S and Ohishi K. Bilateral control using compressor/decompressor under the low-rate communication network. In *IEEE international conference on Mechatronics, 2009 (ICM 2009)*. IEEE, pp. 1–6.
- 28 Kuzu A, Baran EA, Bogosyan S, et al. WPT based compression for bilateral control. In *IECON 2013 - 39th Annual Conference of the IEEE Industrial Electronics Society*. IEEE, pp. 5686–5691.
- 29 Kuzu A, Baran EA, Bogosyan S, et al. Performance comparison of compression techniques used in bilateral control. In *IECON 2013 - 39th annual conference of the IEEE Industrial Electronics Society*. IEEE, pp. 5674–5679.
- 30 Ohnishi K, Shibata M and Murakami T. Motion control for advanced mechatronics. *IEEE/ASME Trans Mechatron* 1996; 1(1): 56–67.
- 31 Saglam CO, Baran EA, Nergiz AO, et al. Model following control with discrete time SMC for time-delayed bilateral control systems. In *2011 IEEE international conference on mechatronics (ICM)*. IEEE, pp. 997–1002.
- 32 Baran EA and Sabanovic A. Predictive input delay compensation for motion control systems. In *2012 12th IEEE international workshop on advanced motion control (AMC)*. IEEE, pp. 1–6.
- 33 Yu J and Karlsson S. Local spectral analysis using wavelet packets. *Circuits Syst Signal Process* 2001; 20(5): 497–528.
- 34 Li Y, Wei Hl and Billings SA. Identification of time-varying systems using multi-wavelet basis functions. *IEEE Trans Control Syst Technol* 2011; 19(3): 656–663.
- 35 Wei D, Bovik AC and Evans BL. Generalized Coiflets: a new family of orthonormal wavelets. In *Conference record of the thirty-first Asilomar conference on signals, systems & computers, 1997, vol. 2*. IEEE, pp. 1259–1263.
- 36 Mallat SG. A theory for multiresolution signal decomposition: the wavelet representation. *IEEE Trans Pattern Anal Machine Intell* 1989; 11(7): 674–693.
- 37 Lee B. Application of the discrete wavelet transform to the monitoring of tool failure in end milling using the spindle motor current. *Int J Adv Manuf Technol* 1999; 15(4): 238–243.
- 38 Beylkin G, Coifman R and Rokhlin V. Fast wavelet transforms and numerical algorithms I. *Commun Pure Appl Math* 1991; 44(2): 141–183.
- 39 Daubechies I. Orthonormal bases of compactly supported wavelets. *Commun Pure Appl Math* 1988; 41(7): 909–996.
- 40 Cohen A, Daubechies I and Feauveau JC. Biorthogonal bases of compactly supported wavelets. *Commun Pure Appl Math* 1992; 45(5): 485–560.
- 41 Karam J. On the zeros of Daubechies orthogonal and biorthogonal wavelets. *Appl Math* 2012; 3(7): 19872.